HHS Public Access

Author manuscript

ACS Appl Bio Mater. Author manuscript; available in PMC 2024 October 07.

Published in final edited form as:

ACS Appl Bio Mater. 2024 August 19; 7(8): 5359–5368. doi:10.1021/acsabm.4c00552.

Interrogating the Role of Endocytosis Pathway and Organelle Trafficking for Doxorubicin-Based Combination Ionic Nanomedicines

Mujeebat Bashiru,
Department of Chemistry, University of Arkansas at Little Rock, Little Rock, Arkansas 72204, United States

Muhammad Rayaan,
Department of Chemistry, University of Arkansas at Little Rock, Little Rock, Arkansas 72204, United States

Nawab Ali,
Department of Biology, University of Arkansas at Little Rock, Little Rock, Arkansas 72204, United States

Samir V. Jenkins,
Department of Radiation Oncology, Winthrop P. Rockefeller Cancer Institute, University of Arkansas for Medical Sciences, Little Rock, Arkansas 72205, United States

Adeniyi Oyebade,
Department of Chemistry, University of Arkansas at Little Rock, Little Rock, Arkansas 72204, United States

Md Shahedur Rahman,
Department of Chemistry, University of Arkansas at Little Rock, Little Rock, Arkansas 72204, United States

Robert J. Griffin,
Department of Radiation Oncology, Winthrop P. Rockefeller Cancer Institute, University of Arkansas for Medical Sciences, Little Rock, Arkansas 72205, United States

Adegboyega K. Oyelere,

Corresponding Author: Noureen Siraj – *Department of Chemistry, University of Arkansas at Little Rock, Little Rock, Arkansas 72204, United States;* nxsiraj@ualr.edu.

Author Contributions

M.B., N.S.: Conceptualization. M.B., N.S.: Data curation. M.B., A.O., S.R., M.R.: Formal analysis. N.S.: Funding acquisition. M. B., M.R.: Investigation. M.B., A.O., S.R., N.S.: Methodology. M.B., N.S.: Project administration. M.B., N.S.: Resources. N.A., N.S.: Supervision. M.B., N.S.: Validation. M.B., S.V.J., N.A., R.J.G., A.K.O., N.S.: Visualization. M.B., Writing. M.B., S.V.J., N. A., R.J.G., A.K.O., N.S.: Writing—review and editing.

The authors declare no competing financial interest.

ASSOCIATED CONTENT

Supporting Information

The Supporting Information is available free of charge at https://pubs.acs.org/doi/10.1021/acsabm.4c00552.

Endocytosis inhibitors; cell viability of endocytic inhibitors; bar graphs showing IC_{50} values, and confocal microscopy images (PDF)

Complete contact information is available at: https://pubs.acs.org/10.1021/acsabm.4c00552

School of Chemistry and Biochemistry, Parker H. Petit Institute for Bioengineering and Bioscience, Georgia Institute of Technology, Atlanta, Georgia 30332, United States

Noureen Siraj
Department of Chemistry, University of Arkansas at Little Rock, Little Rock, Arkansas 72204, United States

Abstract

We have studied the endocytic mechanisms that determine subcellular localization for three carrier-free chemotherapeutic-photothermal (chemo-PTT) combination ionic nanomedicines (INMs) composed of doxorubicin (DOX) and an near-infrared (NIR) dye (ICG, IR820, or IR783). This study aims to understand the cellular basis for previously published enhanced toxicity results of these combination nanomedicines toward MCF-7 breast cancer cells. The active transport mechanism of INMs, unlike free DOX, which is known to employ passive transport, was validated by conducting temperature-dependent cellular uptake of the drug in MCF-7 cells using confocal microscopy. The internalization pathway of these INMs was further probed in the presence and absence of different endocytosis inhibitors. Detailed examination of the mode of entry of the carrier-free INMs in MCF-7 cells revealed that they are primarily internalized through clathrin-mediated endocytosis. In addition, time-dependent subcellular localization studies were also investigated. Examination of time-dependent confocal images indicated that the INMs targeted multiple organelles, in contrast to free DOX that primarily targets the nucleus. Collectively, the high cellular endocytic uptake in cancerous cells (EPR effect) and the multimode targeting ability demonstrated the main reason for the low half-maxima inhibitory concentration (IC_{50}) value (the high cytotoxicity) of these carrier-free INMs as compared to their respective parent chemo and PTT drugs.

Graphical Abstract

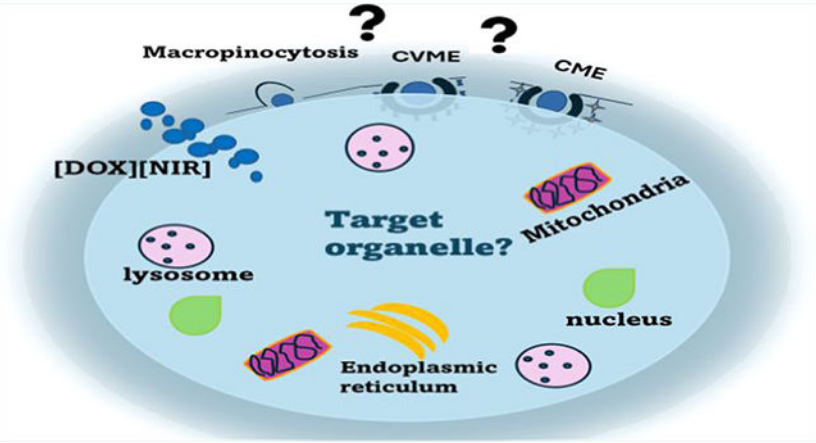

Keywords

ionic nanomaterial; doxorubicin; endocytosis inhibitors; cellular uptake; subcellular localization

1. INTRODUCTION

Nanoparticles have been widely explored for the treatment, immunization, and bioimaging-based diagnosis of diseases.[1,2] Most importantly, the enhanced permeability and retention effect (EPR) exhibited by nanoparticles within tumoral sites makes them suitable to treat cancer.[3] Several studies have demonstrated the loading of active pharmaceutical ingredients (APIs) into nanovehicles such as liposomes, dendrimers, and quantum dots due to their tunable structure, which permits a range of interactions with the cell membrane and efficient encapsulation.[2,4] Even though these nanovehicles are intended to deliver APIs to specific targets, these carriers have little to no therapeutic effect and can also change the absorption, distribution, metabolism, and excretion profile (ADME) of the main APIs.[4,5] Recent research has reported that liposomal formulation of API exhibited reduced therapeutic activity compared to free APIs.[6] This study emphasizes the impact of liposome synthesis method on the particle sizes, drug loading efficiency, and drug release which can alter overall therapeutic activity,[6–8] and thus the importance of carrier-free nanoparticles offering a promising alternative with simple design and straightforward synthesis method that can potentially overcome the limitations associated with traditional nanocarrier systems.[6,9] Carrier-free nanoparticles developed using various methodologies have been utilized to deliver drugs effectively to target organelles owing to the EPR effect within the tumoral site.[10] In a study conducted by Forson et al.,[11] carrier-free porphyrin nanoparticles were designed with positive surface charge to target specific organelles such as the mitochondria.

Internalization of any extracellular material into the cell occurs via active or passive transport. Drugs in the form of macromolecules or particles are actively transported into the cell known as endocytosis.[12] The effectiveness of nanoparticle-based treatments lies in safe entry into the intercellular environment and interaction with the target organelles.[1,13] Numerous nanodrug formulations appear in the literature yearly; however, most of them lack information about their internalization mechanisms, which is critical to evaluate their potential clinical use. To understand the cell-nanoparticle interaction, it is imperative to investigate various possible internalization pathways of the nanoparticles. This could potentially impact the trafficking mechanism that can aid in elucidating the drug's enhanced therapeutic effect.[14]

Commonly known endocytic pathways for nanoparticle internalization are macropinocytosis, clathrin-mediated endocytosis (CME), and caveolin-mediated endocytosis (CVME).[2,15] CME and CVME use specific receptor proteins called "clathrin and caveolin adaptor proteins", responsible for the formation of clathrin or caveolin-coated pits. These specific receptors are found on the cell membrane and allow nanoparticles internalization into the cells.[2,16] This further results in vesicle development, which in turn produces a late endosome (for CME) and caveosome for CVME. For CME, the late endosome fuses with the acidic lysosome to release its content into specific organelles within the cells.[17] However, the caveosome formed during the CVME process leads to the discharge of the content to the endoplasmic reticulum.[18] Although there have been reports that the caveolin-coated vesicle formed during CVME may bypass the lysosomal fusion,[14,19] macropinocytosis is a nonspecific endocytic mechanism that results in the formation of a circular cup vesicle, called the macropinosome through the ruffle invagination of the

membrane.[20,21] The formation of the ruffles allows for engulfment of large particle sizes, leading to macropinosomes, which can subsequently undergo lysosomal fusion.

Doxorubicin, a potent anthracycline drug used to treat many different types of cancer, has a broad therapeutic range.[22,23] The low bioavailability of doxorubicin (DOX) at the target site is due to its low solubility at physiological condition and passive intracellular diffusion.[24] Researchers have employed different carrier approaches such as poly(ethylene glycol) (PEG) or liposomes to enhance the drug's concentration in the cells. Unfortunately, these carrier strategies would not provide enhanced toxicity as compared to free DOX.[8,25,26] Recently, our group utilized a very simple ionic nanomaterial (INM) approach to develop DOX-based combination nanomedicine with high toxicity.[5] These DOX-near-infrared (NIR) INMs were developed and thoroughly characterized. The resulting combination nanomedicines demonstrated improved chemotherapeutic behavior compared to the DOX parent compound.[5] Thus, this study is designed to investigate the possible alterations in the internalization mechanism as well as subcellular localization of DOX-based nanomedicine which provides additional information about the drug's potency, and aid the guidelines necessary for the development of future medications. The literature highlights notable contributions from Warner's group on the development of various INMs.[19,27] However, their group just reported the endocytosis mechanism study only for one rhodamine-based nanomedicine, which was not a combination drug. Moreover, there is no report on the organelle targeting capability of the INMs.[19] In fact, the first study on subcellular localization of porphyrin-based INMs was only published last year by our former colleague.[11] However, this study did not explore the endocytosis mechanisms and did not make any connection between the uptake mechanism and subcellular localization of the INMs. To the best of our knowledge, we are reporting for the first time a time-dependent subcellular localization and endocytosis mechanism of DOX-based combination INMs.

Herein, a detailed study is performed to investigate the internalization mechanism of three distinct INMs ([DOX]-[IR820], [DOX][IR783], and [DOX][ICG]) and parent DOX in MCF-7 breast cancer cells at different temperatures. The changes in the INM's cellular uptake mechanism toward MCF-7 will aid us to understand the effect of DOX's counterions. Endocytosis mechanism of the INMs is further examined through assessment of cellular uptake in the presence and absence of different inhibitors using confocal fluorescence microscopy and a cell viability assay. It is anticipated that INMs physicochemical properties such as nanoparticle sizes, surface charge, and composition play a key role in the endocytosis process which consequently alters their transport mechanisms as opposed to free DOX. Lastly, a time-dependent subcellular localization study of the three INMs, relative to parent DOX was performed to gain more insight into the enhanced therapeutic activity of the INMs.

2. EXPERIMENTAL SECTION

2.1. Chemicals.

Methyl-β-cyclodextrin (MβCD) (lot no. A0374873) was purchased from Acros Organics (New Jersey, NJ). 4-(2-Aminoethyl) benzenesulfonyl fluoride hydrochloride (AEBSF) (lot no. GVPZD-TX) was purchased from Tokyo Chemical Industry (Tokyo, Japan). Filipin III

(lot no. 0000135711), chloropromazine hydrochloride (lot no. MKCN7684), chloroquine diphosphate salt (lot no. 127F-0833), 5-(*N*-ethyl-*N*-isopropyl) amiloride, phosphate-buffered saline (PBS, pH 7.4), and dimethyl sulfoxide (DMSO) were purchased from Sigma-Aldrich. Imipramine hydrochloride (lot no. M09J020) was purchased from Thermo Scientific. Coverslips, paraformaldehyde, glycine, bovine serum albumin (BSA), saponin, glycerol, 1,4-phenylenediamine, and sucrose were purchased from Fisher Scientific (Hanover Park, IL). All chemicals were used as received. Triple deionized water (18.2 MΩ·cm) was obtained using a Purelab Ultrapure water purification system (ELGA, Woodridge, IL). 4′,6-Diamidino-2-phenylindole (DAPI), and both primary LAMP–2 (H4B4) sc-18822 (lot no. L1720) and secondary antibody m-lgGk BP-CFL 488 sc-516176 (lot no. D1922) for lysosome tracker were purchased from Santa Cruz Biotechnology (Texas).

2.2. Synthesis of Ionic Materials (IMs) and Ionic Nanomaterials (INMs).

Three chemotherapeutic-photothermal (chemo-PTT) combination drugs (IMs) were synthesized using a simplistic, rapid, economical, one-step ion exchange method according to previously reported protocol.[5] Briefly, for synthesis of [DOX][IR820] IM, 1:1 mole ratio of DOX and NaIR820 were separately dissolved in water. Aqueous solutions of both DOX and NaIR820 were combined, and the mixture was stirred for 24 h to ensure complete ion exchange reaction. The resultant mixture was centrifuged at 3800 rpm for 5 min, and the supernatant was removed to recover the precipitate of [DOX][IR820] IMs. The precipitate was washed three times with water to remove the byproduct (NaCl). The resultant drug [DOX][IR820] was lyophilized to remove moisture from the IMs before performing further studies. Since NaIR783 and NaICG are also water-soluble dyes, a similar protocol was followed to synthesize the chemo-PTT combination drugs for [DOX][IR783] and [DOX]-[ICG] IMs, respectively. Figure 1 shows the three different NIR dyes, chemodrug, and synthesis scheme for the different chemo-PTT combination IMs.

INMs were prepared by facile reprecipitation method in cell media from IMs for in vitro study.[5] Briefly, a stock solution of the chemo-PTT combination IMs was initially prepared at a 1 mM concentration in DMSO. Next, a small volume of the stock solution was added dropwise to a glass vial containing cell media present in an active sonication bath. The sample was subjected to sonication for 5 min and further stabilized for 20 min before any experiment. A Zetasizer Pro red, Malvern Instruments (Malvern Worcestershire, United Kingdom), was used to determine the hydrodynamic diameter of the INMs in deionized (DI) water by using the dynamic light scattering (DLS) method.

2.3. Cell Culture.

In vitro experiments were performed using the MCF-7 breast cancer cell line obtained from the American Type Culture Collection (ATCC, Manassas, VA). A monolayer of cells was maintained in an incubator at 37 °C and 5% CO_2 in complete cell media. MCF-7 cells were cultured in DMEM supplemented with fetal bovine serum (FBS) (10% v/v) and an antibiotic solution containing penicillin/streptomycin (500 units/mL). When cells reached the desired confluency, they were either subcultured or used for experiments, following trypsination and detachment. The detached cells were washed and stained with trypan blue exclusion dye, followed by counting using a hemocytometer.

2.4. Temperature-Dependent Internalization Study of INMs.

This experiment is designed to determine the potential mode of entry of the drugs (DOX or INMs) into cells as an energy-dependent process or passive uptake. The cells were incubated with INMs or DOX at two temperatures: cold (4 °C) and physiological temperature (37 °C). Active uptake mechanisms such as endocytosis are known to be hindered at low temperatures because it is an energy-dependent process,[17] while passive diffusion cannot be affected by a change in temperature. In a typical experiment, 1.2×10^5 cells per well were plated in a 24-well plate preintroduced with 12 mm circular coverslips. After 24 h incubation, the well plate was further incubated at either temperature (4 or 37 °C) for 1 h before treatment with 5 μM INMs or DOX prepared in cell media. Then, the treated cells were incubated again for an additional 1 h at 4 or 37 °C. Then, the cells were washed thoroughly with phosphate-buffered saline (PBS, pH 7.4) and fixed with 200 μL of paraformaldehyde (4%) for 15 min at room temperature. The cells were post-treated with DAPI (300 nM), a nucleus strainer for 5 min, washed with PBS, and the coverslips were mounted onto microscope slides with 5 μL of mounting media (90% glycerol, 10% PBS with 10 mg 1,4-phenylenediamine). Confocal imaging was performed by using a laser scanning confocal microscope (Zeiss, LSM 880), attached to an inverted microscope. An oil immersion objective lens (63×) was used for cell imaging. A diode excitation source of 405 nm was utilized with the emission set at 650 nm to view INMs.

2.5. Evaluation of Endocytic Uptake Mechanism.

Eight different specific endocytosis inhibitors named Filipin III, sucrose, chlorpromazine, amiloride, imipramine hydrochloride, AEBSF, chloroquine, and MβCD were used to investigate the endocytic routes employed by the INMs on MCF-7 cells. All inhibitors stated have been explored and reported to obstruct endocytosis processes such as CME, CVME, or macropinocytosis. As a result of the nonselectivity of the inhibitors toward a specific endocytic pathway, multiple inhibitors were tested. In a typical experiment, 1.2×10^5 cells were seeded on 12 mm circular coverslips pre-seated in a 24-well plate and incubated for 24 h. After the allotted time, the various endocytosis inhibitors including chlorpromazine, filipin III, sucrose, chloroquine, AEBSF, imipramine hydrochloride, MβCD, and amiloride prepared in cell media were introduced separately into different wells at their respective concentrations for 2 h.[28–31] Table S1 reports the various endocytosis inhibitor as well as their concentrations used in this experiment.[28–31] The excess cell media containing inhibitor was aspirated, and the cells were further treated with 5 μM INMs for an additional 1 h. Next, the cells were washed with PBS and subsequently fixed with 200 μL of paraformaldehyde (4%) for 15 min at room temperature. The coverslips were mounted onto microscope slides with 5 μL of mounting media (90% glycerol, 10% PBS with 10 mg of 1,4-phenylenediamine). Confocal images were taken to view DOX's fluorescence emission using a laser scanning confocal microscope (Zeiss, LSM 880), attached to an inverted microscope.

2.6. Cell Viability Study of Drug in the Presence of Endocytic Inhibitors.

Cells were plated at 1.5×10^4 cells per well in a 96-well plate and incubated at 37 °C and 5% CO_2 for 24 h. The toxicity of the inhibitors was investigated with concentrations

reported in Table S1, and cell viability results are shown in Figure S1. For treatments involving the presence of specific inhibitors, the cells were pretreated with various specific inhibitors for 2 h with indicated inhibitor concentrations (Table S1). The cells were washed with PBS and further treated with INMs prepared in cell media at their half-maxima inhibitory concentration (IC_{50}) and were incubated for 24 h. Cell viability was assessed utilizing the MTT assay. With the use of a microplate reader (Biotek Synergy H1, Winooski, VT), the optical density of the MTT-formazan was determined at 570 nm. Each experiment for in vitro studies was performed in triplicate and repeated three times.

2.7. Subcellular Localization.

Localization experiments were designed to investigate the location of the parent drugs and INMs at the various subcellular organelles at different times. We anticipate that the experiments would aid the understanding of the improved therapeutic effect of INMs as compared to DOX. In a typical experiment, 1.2×10^5 cells per well were seeded in a 24-well plate previously seeded with coverslips and were incubated for 24 h. The cells were washed with PBS, treated, and incubated with the 5 μM INMs or DOX prepared in cell media for 1 or 6 h. After the stated time, the cells were further washed to remove the uninternalized drugs and fixed with paraformaldehyde for 15 min. The cells were then permeabilized using a blocking solution (0.3 M glycine, 10% BSA, 1% saponin in PBS) for 30 min before staining with LAMP antibodies. The cells were incubated with primary LAMP antibody (H4B4) for 30 min at 1:100 dilution according to the manufacturer's protocol. The fixed cells were washed repeatedly thrice with PBS for 5 min intervals totaling 15 min before the addition of the fluorophore-conjugated secondary antibody (Alexa 488) at 1:100 dilution. The cells were washed with PBS and further treated with 300 nM DAPI for 5 min. The cells were washed with PBS before mounting on the glass slide and imaged using a laser scanning confocal microscope (Zeiss, LSM 880). Quantitative analysis was performed by creating a region of interest around the whole cell and the nucleus. The total area of the drug content (red channel) in the whole cell and the nucleus was also obtained from the Zeiss LSM 880 instrument. The colocalization of the drug with LAMP 2 was also acquired.

3. RESULTS AND DISCUSSION

Based on our previous findings, it was observed that the synthesized INMs are spherical in shape.[5] Their hydrodynamic diameters are 54.1 + 22.5, 171.1 ± 30, and 56 ± 30 nm for [DOX][IR820], [DOX][IR783], and [DOX][ICG], respectively. The cell viability results from our previous study in MCF-7 showed that the three INMs had much lower IC_{50} values, and are therefore more cytotoxic than DOX.[5] The IC_{50} values for the DOX and various INMs are shown in Figure S2. Moreover, caspase and flow cytometry analysis revealed that INMs caused more apoptotic cell death than free soluble DOX.[5]

3.1. Affirming Endocytic Uptake for INMs.

To understand the enhanced dark toxicity and improved apoptotic cell death mechanisms, the cellular uptake mechanism was studied in detail. Literature reports have confirmed that soluble drugs employ passive transport mechanism to internalize into the cells.[13,16,32] However, when these drugs were incorporated into the nanoparticles for drug delivery

purpose, the nanoparticles mainly utilized endocytosis mechanism for internalization into the cells.[19,29] To investigate the potential uptake mechanism of the DOX-based INMs and the parent DOX drug, the cells were incubated with the drug as stated in the experimental section at two different temperature conditions (4 and 37 °C). These two temperatures were selected because passive uptake mechanism does not depend on temperature while it is well established that active transport is usually hindered at low temperatures.[19] After 1 h post treatment, the cells were examined using confocal microscopy. It was observed that only the parent DOX, the soluble chemotherapeutic drug was internalized into the MCF-7 cells at both temperatures, as evident from the fluorescence emission of DOX (Figure 2, green arrow showing uptake at low temperature) inside the cell. This indicates that DOX is being passively uptaken by the cell since the DOX uptake is not affected by the temperature condition. However, the fluorescence emission of all INMs was observed in the cells at only the physiological temperature (37 °C) condition but not at a low temperature (4 °C). This observation proved that these soft carrier-free INMs utilized active transport mechanisms to internalize into the cells. The difference in the uptake mechanism could be the reason for enhanced cytotoxicity and improved apoptosis mechanism.

3.2. Endocytosis Inhibitor Assay.

Since INMs employed active transport mechanisms, it is important to investigate the endocytosis mechanisms of all INMs to better understand their improved cytotoxicity toward MCF-7 cells as compared to the parent DOX. Macropinocytosis, CVME, and CME are all size-dependent endocytosis mechanisms,[1] with internalized nanoparticle sizes of 0.2–5 μm, 50–100 nm, and less than 200 nm, respectively.[1,33,34]

Since not all endocytic pathways can be deduced by using a single inhibitor due to its nonselectivity, more than one inhibitor was utilized to verify the endocytic route of each INMs. Table 1 lists the various endocytosis inhibitors that have been studied along with the blocked routes. In addition, the cell viability of the different endocytic inhibitors is also reported in Figure S1. The results obtained for each INM are presented one by one. First, the endocytosis path of [DOX][IR820] INM is presented. Amiloride, a macropinocytosis known inhibitor, was first used to examine the macropinocytosis pathway. When [DOX][IR820] INMs were introduced to MCF-7 cells pretreated with amiloride (Figure 3), the internalization of [DOX][IR820] INMs into the cells was not hindered, as evident by confocal fluorescence images showing no significant decrease in the cellular uptake of the nanodrug. This observation was validated with a different macropinocytosis inhibitor: imipramine. As seen with amiloride, imipramine caused no change in fluorescence emission of [DOX][IR820] INMs. These results demonstrate that [DOX][IR820] INMs do not employ macropinocytosis as their mode of entry into the MCF-7 cells.

Next, a filipin III inhibitor was used to investigate the CVME process as a possible mechanism for the uptake of [DOX][IR820] INMs. It is well known that filipin III blocks majorly CVME endocytosis pathway with its mode of action focusing on cholesterol binding.[29,35] Filipin III has also been reported to obstruct the CME pathway.[29,35] It was observed that the cellular uptake of [DOX][IR820] INMs was slightly reduced in the presence of the filipin III inhibitor as shown in Figure 4. However, a decrease in the

fluorescence emission of the drug could imply that the drug is being internalized by more than one pathway. Thus, indicating that the entry of [DOX][IR820] INMs in MCF-7 cells could be CVME-dependent in addition to other possible mechanisms such as CME.

To further investigate whether [DOX][IR820] INMs were actively endocytosed via the CME mechanism, the effect of a CME known inhibitor such as MβCD on drug internalization (Figure 5a) toward MCF-7 cells was examined. It is important to clarify that MβCD is known to nonselectively inhibit multiple pathways such as CME and CVME. The confocal fluorescence images revealed a slight decrease in the fluorescence emission of the [DOX][IR820] INMs, signifying the possibility of CME and CVME pathways as the mode of entry in MCF-7 cells. CME mechanism was also investigated using sucrose as an inhibitor. Hypertonic sucrose is known to hinder the clathrin-coated pit formation, thereby hindering the CME process.[2,36] It was observed that the uptake of [DOX][IR820] INMs in MCF-7 cells decreased with treatment involving sucrose when compared with that of the control (Figure 5b). Next, the cellular uptake of [DOX]-[IR820] INMs in the presence of chlorpromazine, majorly known to inhibit the CME process, was examined. It was observed that the fluorescence emission of the drug was quenched, as depicted by a reduced uptake of INMs (Figure 5c). We also quantitatively analyzed the average fluorescence emission of the INMs in the presence of CME, CVME, and macropinocytosis known inhibitors and presented the bar graphs in Figure 6. Both quantitative and qualitative results indicate the likely endocytosis pathway of [DOX][IR820] to be CME. Based on the size of [DOX][IR820] INMs, i.e., 54.1 ± 22.5 nm, it is expected to be internalized via either CME or CVME routes.

Similar endocytic inhibitors were examined for the endocytosis mechanism employed by the [DOX][IR783] INMs in MCF-7 cells. The cellular uptake of [DOX][IR783] was not affected in the presence of amiloride inhibitor (Figure S3). However, there was a decrease in the uptake of nanodrugs in the presence of imipramine. As stated earlier, there have been some controversies on imipramine's ambiguous mechanism.[29] Nevertheless, other studies indicate that imipramine blocks macropinocytosis route.[37] Based on this result as well as its size (nearly 200 nm), it is possible that [DOX][IR783] INMs are being endocytosed via the macropinocytosis route.

Next, the relationship between [DOX][IR783] INMs and the CME process was studied. When MCF-7 cells were pretreated with MβCD inhibitor prior to [DOX][IR783] INMs, the fluorescence emission of [DOX][IR783] INMs was not altered (Figure S4a). It is well known that MβCD may also inhibit other processes such as CVME pathway in addition to the CME process.[1,34] In the presence of chlorpromazine, known to majorly impede the CME process, there was a slight reduction in the uptake of [DOX][IR783] INM in MCF-7 as shown in Figure S4b. Although it has been reported that chlorpromazine can inhibit CVME pathway in addition to CME (Table 1), when MCF-7 cells pretreated with sucrose were treated with [DOX][IR783], we observed only a slight decrease in the cellular uptake of [DOX][IR783] (Figure S4c). Hypertonic sucrose is known to nonselectively obstruct both CME and macropinocytosis routes. This ambiguity informed our decision to further investigate the role of the CVME process in the internalization of [DOX][IR783] INMs using filipin III, which obstructs both the CVME and CME routes. Interestingly, the cell

uptake of [DOX][IR783] on MCF-7 cells was reduced upon treatment with filipin III, as evident from the images shown in Figure S5. Based on the nanoparticle size range (171.1 ± 30 nm) and complexity of [DOX][IR783] INMs uptake mechanism, it is evident that [DOX][IR783] INMs employ more than one endocytosis route including macropinocytosis, CME and CVME.

For the endocytic study involving [DOX][ICG] INMs in the presence of a macropinocytosis inhibitor, both amiloride and imipramine did not impact the internalization process (Figure S6). Similarly, upon treatment of [DOX][ICG] with MCF-7 cells in the presence of filipin III (a CVME inhibitor), there was only a slight decrease in the cell uptake of the nanodrug, as shown in Figure S7. The cellular uptake of [DOX][ICG] INMs was not reduced when the cells were treated with the MβCD inhibitor prior to the [DOX][ICG] introduction in the MCF-7 cells (Figure S8). However, confocal fluorescence images revealed that the presence of chlorpromazine and sucrose only marginally decreased the level of cell uptake of [DOX][ICG] INMs (Figure S8b,c). These inhibitors are known to majorly obstruct the CME in addition to the CVME pathway. As previously stated, the introduction of a specific type of inhibitor may also lead to the modulation of other pathways alongside their major pathway. For instance, a specific inhibitor such as sucrose known to majorly inhibit the CME route has also been reported to have some off-target effects leading to the uptake of drugs via macropinocytosis due to possible crosstalk between different endocytosis pathways.[1] It is not new that one nanodrug may use two different endocytosis pathways for the cell internalization process. In addition, Sousa et al., reported that macropinocytosis is a nonspecific cargo uptake mechanism and does not solely depend on the size of the nanoparticle.[29]

Detailed examination of the confocal images revealed that the internalization pathway of the three INMs involved at least CME and other additional endocytosis pathways. It is interesting to note that simply by changing the counterion, the endocytosis mechanism can be tuned. When particles are endocytosed via the CME process, it is anticipated that the nanoparticle will fuse with the lysosome at a later stage of the process, following the development of the late endosome. Therefore, to further comprehend the internalization processes of these DOX-based INMs in MCF-7 cells, the role of specific lysosomal inhibitors and lysosomal enzyme in MCF-7 cells was examined upon treatment with the INMs.[19] Chloroquine is a commonly known lysosomal inhibitor that reduces the lysosome activity and inhibits the CME process. On the other hand, a lysosomal enzyme like AEBSF can increase lysosomal activity.[19] When MCF-7 cells were treated independently with the three INMs in the presence of chloroquine, there was a significant decrease in the fluorescence emission of the three INMs as compared to the control (Figure S9). This suggests the possible pathway for [DOX][IR820], [DOX][IR783], and [DOX][ICG] INMs internalization involves the CME process. In the case of AEBSF lysosomal enzyme, it was observed that the presence of AEBSF did not cause a decrease in the cellular uptake of the three INMs toward MCF-7. This would mean that the increased lysosomal activity led to enhanced lysosomal fusion (Figure S9). Thus, the confocal imaging result signifies that the internalization process of [DOX][IR820] and [DOX][IR783] INMs occurs via the CME pathway.

3.3. In Vitro Cell Viability Study in the Presence of Endocytosis Inhibitors.

The complicated uptake mechanism employed by some of the INMs led us to validate the results by using a quantitative cell viability assay. We have investigated the toxicity of DOX-based INMs on MCF-7 breast cancer cells in our previous report.[5] A change in cell viability in the presence of an endocytosis inhibitor would depict a possible pathway for the uptake process. Cell viability results shown in Figure 7 revealed that the toxicity of [DOX][IR820] INMs decreased in the presence of CME-related inhibitors (chlorpromazine, sucrose, and chloroquine) in relation to the control (drug only without inhibitor). All of these CME inhibitors decreased the uptake of [DOX][IR820] INMs. MCF-7 cells pretreated with chlorpromazine prior to [DOX]-[IR820] incubation resulted in the lowest cellular uptake of the nanodrug when compared to treatments involving other inhibitors. This result signifies cell growth due to complete obstruction of the CME pathway caused by chlorpromazine. This result agrees with the confocal fluorescence image earlier discussed for [DOX][IR820] INMs shown in Figure 5c. Cell viability results involving filipin III-treated MCF-7 cells incubated with [DOX][IR820] INMs similarly showed a decreased cellular uptake. This data signifies the inhibitory effect of CVME, in addition to the major CME pathway employed by the nanodrug as a means of internalization in MCF-7. However, AEBSF-treated MCF-7 cells showed no significant difference in the cellular uptake of [DOX][IR820] INMs concerning the drug treatment only. This result is consistent with the fluorescence images shown in Figure S9. In the presence of macropinocytosis-related inhibitors such as imipramine and amiloride, we observed some inhibitory effects with imipramine only but not with amiloride. The effect exhibited with treatment involving imipramine could possibly be due to its unclear mechanism of endocytosis previously reported.[29] Therefore, both quantitative confocal fluorescence imaging and qualitative cell viability results demonstrated the primary involvement of the CME in addition to a secondary CVME for [DOX][IR820] INMs in MCF-7 cells.

Cell viability results for MCF-7 cells treated with [DOX]-[IR783] INMs in the presence of different endocytic inhibitors are reported in Figure S10. These results revealed that the presence of CME-related inhibitors (chlorpromazine, sucrose, chloroquine, and MβCD) reduced the cellular uptake of [DOX][IR783] INMs in MCF-7, thus rendering the nanodrug less toxic. Thus, the results confirmed that [DOX][IR783] employs the CME pathway as a means of entry into MCF-7 cells. We also observed that filipin III also hindered the internalization of [DOX][IR783] INMs and thus led to increased cell viability. The lowest cellular uptake was exhibited with the treatment involving [DOX][IR783] INMs in the presence of macropinocytosis inhibitors such as imipramine and amiloride, possibly indicating partial cellular uptake via the macropinocytosis route. These results demonstrated that [DOX][IR783] INMs employed the CME and CVME pathways for internalization in MCF-7 cells.

When MCF-7 cells, preincubated with the different endocytosis inhibitors chlorpromazine, sucrose, and chloroquine, were post-treated with [DOX][ICG] INMs, we observed a reduction in the cellular uptake of [DOX][ICG] in comparison with the [DOX][ICG] treatment in the absence of these endocytosis inhibitors (control) (Figure S11). Similarly, the presence of filipin III also resulted in increased cell viability results. However, treatment

involving other inhibitors such as imipramine, AEBSF, MβCD, and amiloride did not significantly alter the cellular uptake in MCF-7 cells. Therefore, the study demonstrated the partial involvement of CME or CVME in the uptake of [DOX][ICG] by the MCF-7 cells.

3.4. Subcellular Localization.

After identifying the endocytosis pathway for each INMs, it is important to investigate the final location of the drug in the subcellular organelles which can provide a better insight into the improved toxicity of the drug. In the subcellular localization study, the parent DOX drug was also included as control to investigate any changes of the DOX-based INM's target in the cells. To investigate the subcellular localization of the combination drugs in MCF-7 cells, confocal imaging was performed. The localization of the soluble chemodrug and the various chemo-PTT INMs within the cell was investigated at different times (1 and 6 h). Confocal imaging is effective for observing drug's localization at the subcellular level based on the drug emission, which could also reveal the potential organelle subjected to damage and ultimately responsible for cell death.

Qualitative and quantitative confocal imaging results presented in Figures 8 and 9 revealed that DOX was mainly concentrated in the nucleus for the first hour as evidenced by the overlap of the DOX's red emission with DAPI. The DOX remained localized in the nucleus even after 6 h of drug incubation (with no drug colocalized with LAMP 2), corroborating earlier research about the DOX targeting the nucleus.[38] It is well established that DOX inhibits topoisomerase II which hinders DNA repair processes and causes apoptosis.[5] [DOX][IR820] INM was observed mainly within the nucleus for the first hour of incubation. It is interesting to note that [DOX][IR820] INM's location changed over time. After 6 h, it was observed to be present in both the nucleus and the lysosome, as evidenced by the INMs intense emission overlapping with the LAMP 2 antibody. Similarly, throughout the first hour, [DOX][IR783] and [DOX][ICG] INMs primarily targeted the cell's nucleus. As incubation time increased, the [DOX][ICG] INMs targets shifted to the cell's lysosome. However, the cellular uptake of [DOX][IR783] decreases with time due to the nanoparticle morphology. [DOX][IR783] cellular uptake was more in the first hour as compared to 6 h (as evident from both qualitative and quantitative results (Figures 8 and 9)). A shift in the location of the INMs indicates the effect of the DOX counterion and its nanoparticle morphology that impacted its subcellular localization. The cellular uptake and changes in subcellular localization of INMs as compared to parent DOX are attributed to the improved toxicity as well as enhanced apoptosis mechanism of the INMs. According to reports, lysosome destruction triggers apoptosis by releasing proteolytic enzymes into the cytoplasm.[39] It is important to note that all confocal images were recorded at a DOX emission wavelength. Unfortunately, the unavailability of NIR confocal imaging facilities restricted us from tracking the NIR dyes in the INMs. Although previous research reports the localization of cyanine dyes such as NaIR783 within the lysosome.[40] It is possible that NIR counterions are dragging the DOX toward lysosome and improving the apoptosis cell death mechanism of the overall drug. Consequently, the location of the drug in both nucleus and lysosome can enhance the therapeutic effect on the cancer cell.[41] In addition, these results also demonstrated the stability of INMs in the cells since DOX emission in INMs changed over time, while the parent DOX stayed in the nucleus only. Relative to DOX,

Chemo-PTT INMs offer the benefits of multimodal organelle targeting that enhanced not only their toxicity but also their apoptotic cell death mechanisms. These results could be tremendously important toward addressing the side effects of the DOX. In the future, we will present a more detailed study of different cell lines and organelles to explore the full potential of INMs.

4. CONCLUSIONS

In summary, energy-dependent active transport mechanisms are being employed by three distinct INMs toward MCF-7 cells as opposed to free soluble DOX that exhibited passive uptake. The alteration in the INMs internalization process is attributed to the effect of DOX counterions and nanoparticle morphology. INMs employ CME as their primary means of internalization, in addition to other secondary endocytic pathways such as CVME. [DOX][IR820] INMs showed principal internalization via CME due to the drastic quenching of the fluorescence emission of the drug, as well as increased cell viability of the cells in the presence of CME inhibitors. While [DOX][IR783] employed CME, CVME, and macropinocytosis pathways as a means of entry into MCF-7 cells, [DOX][ICG] exhibited a more complicated endocytic mechanism with partial internalization using the CME or CVME route. Time-dependent subcellular studies for all INMs revealed that the INMs are concentrated in multiple organelles over time (nucleus and lysosome) as opposed to soluble DOX that majorly localizes in the nucleus. This dual organelle-targeted INMs provides a promising strategy to improve the therapeutic activity of the drug toward cancer cells.

Supplementary Material

Refer to Web version on PubMed Central for supplementary material.

ACKNOWLEDGMENTS

This publication was made possible by the Arkansas INBRE program, supported by a grant from the National Institute of General Medical Sciences, (NIGMS), P20 GM103429 from the National Institutes of Health. N.S. gratefully acknowledges financial support through the National Science Foundation EPSCoR Research Infrastructure under award number RII Track 4–1833004. Any opinions, findings, and conclusions or recommendations expressed in this material are those of the author(s) and do not necessarily reflect the views of the National Institute of Health or the National Science Foundation.

REFERENCES

(1). Rennick JJ; Johnston APR; Parton RG Key Principles and Methods for Studying the Endocytosis of Biological and Nanoparticle Therapeutics. Nat. Nanotechnol. 2021, 16 (3), 266–276. [PubMed: 33712737]

(2). Sahay G; Alakhova DY; Kabanov AV Endocytosis of Nanomedicines. J. Controlled Release 2010, 145 (3), 182–195.

(3). Kalyane D; Raval N; Maheshwari R; Tambe V; Kalia K; Tekade RK Employment of Enhanced Permeability and Retention Effect (EPR): Nanoparticle-Based Precision Tools for Targeting of Therapeutic and Diagnostic Agent in Cancer. Mater. Sci. Eng.: C 2019, 98, 1252–1276.

(4). Macchi S; Jalihal A; Hooshmand N; Zubair M; Jenkins S; Alwan N; El-Sayed M; Ali N; Griffin RJ; Siraj N Enhanced Photothermal Heating and Combination Therapy of NIR Dye via Conversion to Self-Assembled Ionic Nanomaterials. J. Mater. Chem. B 2022, 10 (5), 806–816. [PubMed: 35043823]

(5). Bashiru M; Macchi S; Forson M; Khan A; Ishtiaq A; Oyebade A; Jalihal A; Ali N; Griffin RJ; Oyelere AK; et al. Doxorubicin-Based Ionic Nanomedicines for Combined Chemo-Phototherapy of Cancer. ACS Appl. Nano Mater. 2024, 7 (2), 2176–2189. [PubMed: 38410412]

(6). Mendez-Pfeiffer P; Juarez J; Hernandez J; Taboada P; Virués C; Valencia D; Velazquez C Nanocarriers as Drug Delivery Systems for Propolis: A Therapeutic Approach. J. Drug Delivery Sci. Technol. 2021, 65, No. 102762, DOI: 10.1016/j.jddst.2021.102762.

(7). Hossen S; Hossain MK; Basher MK; Mia MNH; Rahman MT; Uddin MJ Smart Nanocarrier-Based Drug Delivery Systems for Cancer Therapy and Toxicity Studies: A Review. J. Adv. Res. 2019, 15, 1–18. [PubMed: 30581608]

(8). Shim MK; Park J; Yoon HY; Lee S; Um W; Kim JH; Kang SW; Seo JW; Hyun SW; Park JH; et al. Carrier-Free Nanoparticles of Cathepsin B-Cleavable Peptide-Conjugated Doxorubicin Prodrug for Cancer Targeting Therapy. J. Controlled Release 2019, 294, 376–389.

(9). Karaosmanoglu S; Zhou M; Shi B; Zhang X; Williams GR; Chen X Carrier-Free Nanodrugs for Safe and Effective Cancer Treatment. J. Controlled Release 2021, 329, 805–832, DOI: 10.1016/j.jconrel.2020.10.014.

(10). Wang X; Qiu Y; Wang M; Zhang C; Zhang T; Zhou H; Zhao W; Zhao W; Xia G; Shao R Endocytosis and Organelle Targeting of Nanomedicines in Cancer Therapy. Int. J. Nanomed. 2020, 15, 9447–9467.

(11). Forson M; Bashiru M; Macchi S; Singh S; Anderson AD; Sayyed S; Ishtiaq A; Griffin R; Ali N; Oyelere AK; et al. Cationic Porphyrin-Based Ionic Nanomedicines for Improved Photodynamic Therapy. ACS Appl. Bio Mater. 2023, 6 (12), 5662–5675.

(12). Duncan R; Richardson SCW Endocytosis and Intracellular Trafficking as Gateways for Nanomedicine Delivery: Opportunities and Challenges. Mol. Pharmaceutics 2012, 9 (9), 2380–2402.

(13). Patel S; Kim J; Herrera M; Mukherjee A; Kabanov AV; Sahay G Brief Update on Endocytosis of Nanomedicines. Adv. Drug Delivery Rev. 2019, 144, 90–111.

(14). Behzadi S; Serpooshan V; Tao W; Hamaly MA; Alkawareek MY; Dreaden EC; Brown D; Alkilany AM; Farokhzad OC; Mahmoudi M Cellular Uptake of Nanoparticles: Journey inside the Cell. Chem. Soc. Rev. 2017, 46 (14), 4218–4244. [PubMed: 28585944]

(15). Fu X; Shi Y; Qi T; Qiu S; Huang Y; Zhao X; Sun Q; Lin G Precise Design Strategies of Nanomedicine for Improving Cancer Therapeutic Efficacy Using Subcellular Targeting. Signal Transduction Targeted Ther. 2020, 5 (1), No. 262.

(16). Miaczynska M; Stenmark H Mechanisms and Functions of Endocytosis. J. Cell Biol. 2008, 180 (1), 7–11. [PubMed: 18195098]

(17). Lv C; Yang C; Ding D; Sun Y; Wang R; Han D; Tan W Endocytic Pathways and Intracellular Transport of Aptamer-Drug Conjugates in Live Cells Monitored by Single-Particle Tracking. Anal. Chem. 2019, 91 (21), 13818–13823. [PubMed: 31593429]

(18). Manzanares D; Ceña V. Endocytosis: The Nanoparticle and Submicron Nanocompounds Gateway into the Cell. Pharmaceutics 2020, 12 (4), No. 371. [PubMed: 32316537]

(19). Bhattarai N; Mathis JM; Chen M; Pérez RL; Siraj N; Magut PKS; McDonough K; Sahasrabudhe G; Warner IM Endocytic Selective Toxicity of Rhodamine 6G NanoGUMBOS in Breast Cancer Cells. Mol. Pharmaceutics 2018, 15 (9), 3837–3845.

(20). Lin XP; Mintern JD; Gleeson PA Macropinocytosis in Different Cell Types: Similarities and Differences. Membranes 2020, 10 (8), No. 177. [PubMed: 32756454]

(21). Kay RR Macropinocytosis: Biology and Mechanisms. Cells Dev. 2021, 168, No. 203713. [PubMed: 34175511]

(22). Sun C; Zhou L; Gou M; Shi S; Li T; Lang J Improved Antitumor Activity and Reduced Myocardial Toxicity of Doxorubicin Encapsulated in MPEG-PCL Nanoparticles. Oncol. Rep. 2016, 35 (6), 3600−3606. [PubMed: 27109195]

(23). Injac R; Strukelj B Recent Advances in Protection against Doxorubicin-Induced Toxicity. Technol. Cancer Res. Treat. 2008, 7 (6), 497–516. [PubMed: 19044329]

(24). Feng H; Chu D; Li Z; Guo Z; Jin L; Fan B; Zhang J; Li J A DOX-Loaded Polymer Micelle for Effectively Inhibiting Cancer Cells. RSC Adv. 2018, 8 (46), 25949–25954. [PubMed: 35541975]

(25). Lee J; Choi MK; Song IS Recent Advances in Doxorubicin Formulation to Enhance Pharmacokinetics and Tumor Targeting. Pharmaceuticals 2023, 16 (6), No. 802, DOI: 10.3390/ph16060802. [PubMed: 37375753]

(26). Lai PS; Lou PJ; Peng CL; Pai CL; Yen WN; Huang MY; Young TH; Shieh MJ Doxorubicin Delivery by Polyamidoamine Dendrimer Conjugation and Photochemical Internalization for Cancer Therapy. J. Controlled Release 2007, 122 (1), 39–46.

(27). Bhattarai N; Chen M; Pérez RL; Ravula S; Chhotaray P; Hamdan S; McDonough K; Tiwari S; Warner IM Enhanced Chemotherapeutic Toxicity of Cyclodextrin Templated Size-Tunable Rhodamine 6G NanoGUMBOS. J. Mater. Chem. B 2018, 6 (34), 5451–5459. [PubMed: 32254604]

(28). Schnitzer JE; Oh P; Pinney E; Allard J Filipin-Sensitive Caveolae-Mediated Transport in Endothelium: Reduced Transcytosis, Scavenger Endocytosis, and Capillary Permeability of Select Macromolecules. J. Cell Biol. 1994, 127 (5), 1217–1232. [PubMed: 7525606]

(29). De Almeida MS; Susnik E; Drasler B; Taladriz-Blanco P; Petri-Fink A; Rothen-Rutishauser B Understanding Nanoparticle Endocytosis to Improve Targeting Strategies in Nanomedicine. Chem. Soc. Rev. 2021, 50 (9), 5397–5434. [PubMed: 33666625]

(30). Wolfram J; Nizzero S; Liu H; Li F; Zhang G; Li Z; Shen H; Blanco E; Ferrari M A Chloroquine-Induced Macrophage-Preconditioning Strategy for Improved Nanodelivery. Sci. Rep. 2017, 7 (1), No. 13738. [PubMed: 29062065]

(31). Rodal SK; Skretting G; Garred O; Vilhardt F; van Deurs B; Sandvig K Extraction of cholesterol with methyl-beta-cyclodextrin perturbs formation of clathrin-coated endocytic vesicles. Mol. Biol. Cell 1999, 10 (4), 961–974. [PubMed: 10198050]

(32). Li R; Zheng K; Yuan C; Chen Z; Huang M Be Active or Not: The Relative Contribution of Active and Passive Tumor Targeting of Nanomaterials. Nanotheranostics 2017, 1 (4), 346–357. [PubMed: 29071198]

(33). Akinc A; Battaglia G Exploiting Endocytosis for Nanomedicines. Cold Spring Harbor Perspect. Biol. 2013, 5 (11), No. a016980, DOI: 10.1101/cshperspect.a016980.

(34). Hessien M; Donia T; Tabll AA; Adly E; Abdelhafez TH; Attia A; Alkafaas SS; Kuna L; Glasnovic M; Cosic V; et al. Mechanistic-Based Classification of Endocytosis-Related Inhibitors: Does It Aid in Assigning Drugs against SARS-CoV-2? Viruses 2023, 15 (5), No. 1040. [PubMed: 37243127]

(35). Dutta D; Donaldson JG Search for Inhibitors of Endocytosis. Cell. Logist. 2012, 2 (4), 203–208. [PubMed: 23538558]

(36). Kitchens KM; Kolhatkar RB; Swaan PW; Ghandehari H Endocytosis Inhibitors Prevent Poly(Amidoamine) Dendrimer Internalization and Permeability across Caco-2 Cells. Mol. Pharmaceutics 2008, 5 (2), 364–369.

(37). Ju Y; Guo H; Edman M; Hamm-Alvarez SF Application of Advances in Endocytosis and Membrane Trafficking to Drug Delivery. Adv. Drug Delivery Rev. 2020, 157, 118–141.

(38). Suarasan S; Focsan M; Potara M; Soritau O; Florea A; Maniu D; Astilean S Doxorubicin-Incorporated Nanotherapeutic Delivery System Based on Gelatin-Coated Gold Nanoparticles: Formulation, Drug Release, and Multimodal Imaging of Cellular Internalization. ACS Appl. Mater. Interfaces 2016, 8 (35), 22900–22913. [PubMed: 27537061]

(39). Fennelly C; Amaravadi RK Lysosomal Biology in Cancer. In Lysosomes: Methods and Protocols; Springer, 2017; Vol. 1594, pp 293–308.

(40). Yang X; Shi C; Tong R; Qian W; Zhau HE; Wang R; Zhu G; Cheng J; Yang VW; Cheng T; et al. Near IR Heptamethine Cyanine Dye-Mediated Cancer Imaging. Clin. Cancer Res. 2010, 16 (10), 2833–2844. [PubMed: 20410058]

(41). Zhuang J.; Li N.; Zhang Y.; Li B.; Wen H.; Zhang X.; Zhang T.; Zhao N.; Tang BZ. Esterase-Activated Theranostic Prodrug for Dual Organelles-Targeted Imaging and Synergetic Chemo-Photodynamic Cancer Therapy. CCS Chem. 2022, 4 (3), 1028–1043.

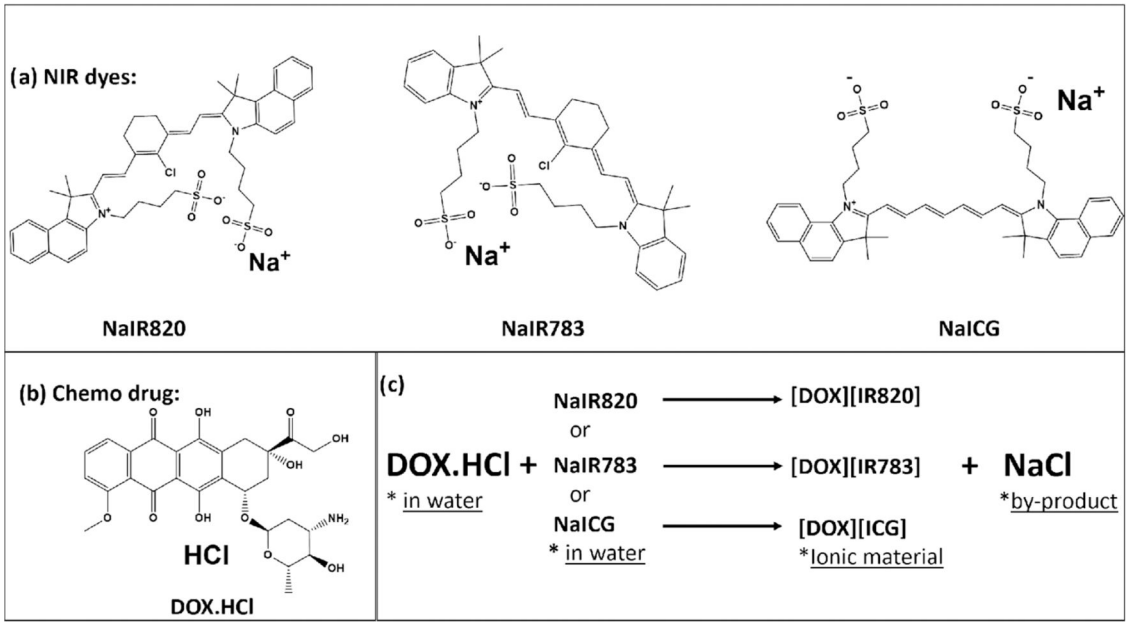

Figure 1.

(a) Structure of NIR dyes. (b) Structure of DOX chemotherapeutic drug used for IMs synthesis. (c) Synthesis scheme for the three chemo-PTT combination IMs.

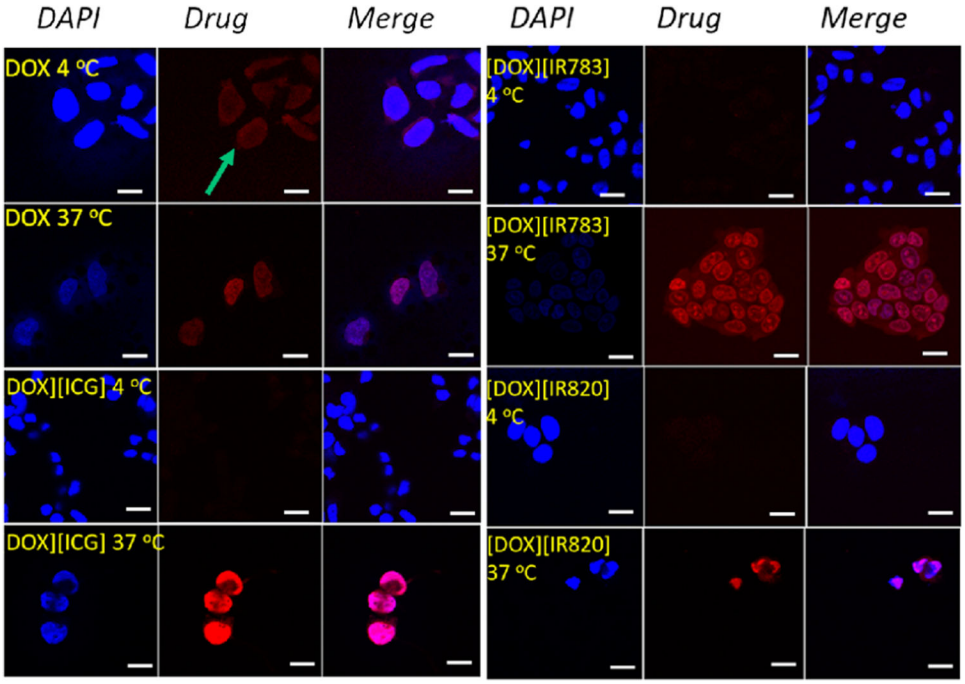

Figure 2.

Confocal microscopy images showing the internalization of DOX and DOX-based INMs recorded at two different temperatures (4 and 37 °C) in MCF-7 cells. Drugs were introduced at 5 μM concentration and incubated for 1 h. Scale bar = 10 μm.

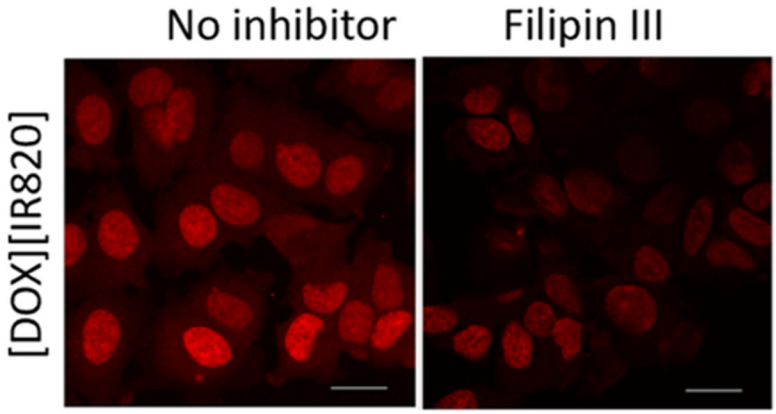

Figure 3.

Confocal microscopy images of macropinocytosis inhibitor-treated MCF-7 cells incubated with [DOX][IR820] INMs. Cells were incubated with amiloride and imipramine at 5 μM and 12.6 μM, respectively, prior to drug treatment. Scale bar represents 10 μm.

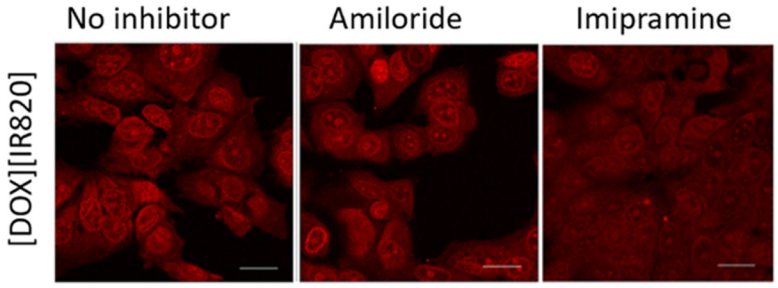

Figure 4.

Confocal microscopy images of [DOX][IR820] INMs-treated MCF-7 cells in the presence of filipin III, a CVME-related inhibitor, introduced at a 4.6 mM concentration. Scale bar represents 10 μm.

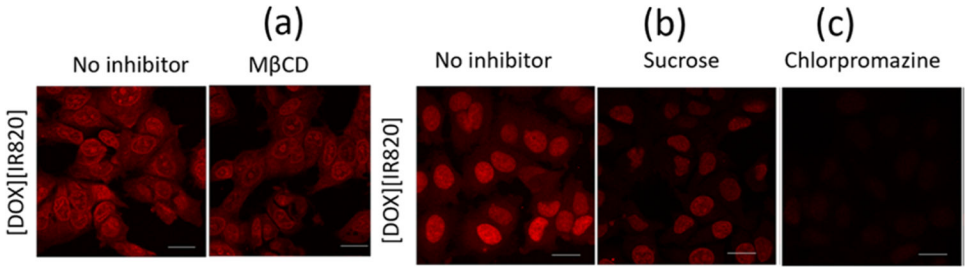

Figure 5.

Confocal microscopy images of CME-related inhibitor-treated MCF-7 cells incubated with [DOX][IR820] INMs. (a) MβCD, (b) sucrose, and (c) chlorpromazine. Cells were incubated with MβCD, sucrose, and chlorpromazine at 2.5 μM, 0.3 mM, and 21.9 μM, respectively. Scale bar represents 10 μm.

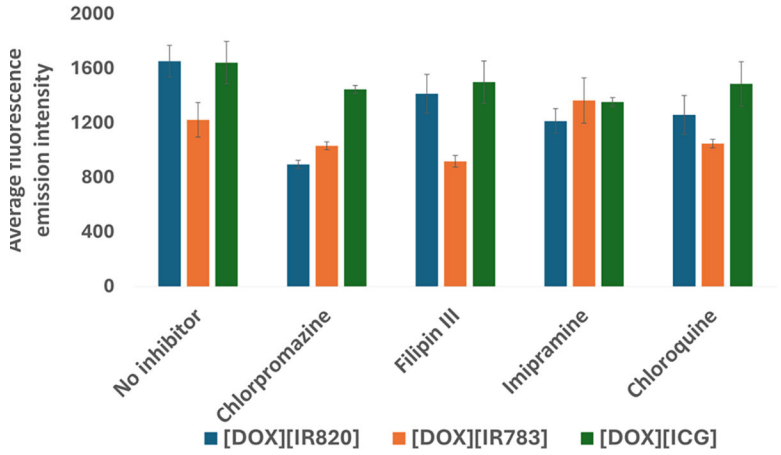

Figure 6.

Quantitative measurement of the average fluorescence emission of three INMs in the presence of chlorpromazine, filipin III, imipramine, and chloroquine known for CME, CVME, macropinocytosis, and CME inhibition, respectively.

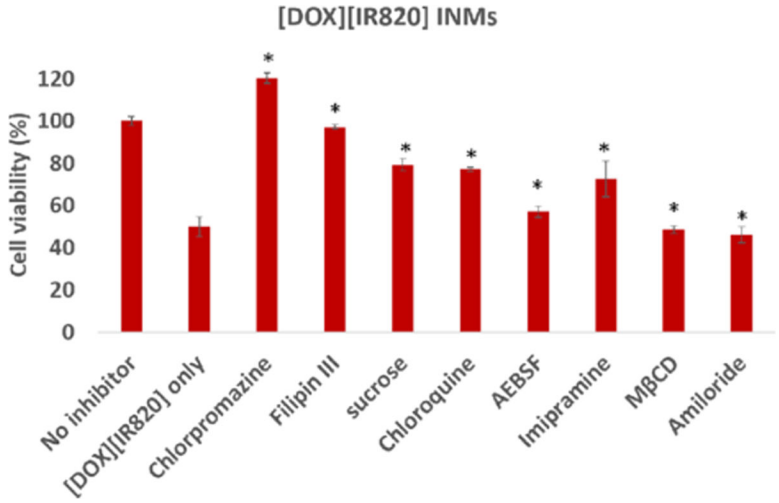

Figure 7.

Cell viability of [DOX][IR820] INMs in MCF-7 cells in the presence of different endocytosis inhibitors preincubated for 2 h at 37 °C prior to drug exposure for 24 h. Cells were exposed to [DOX][IR820] INMs at 0.74 μM.[5] The results are represented as mean ± SD ($n = 3$), statistically significant $p \leq 0.05$ (*) was evaluated using the student t test.

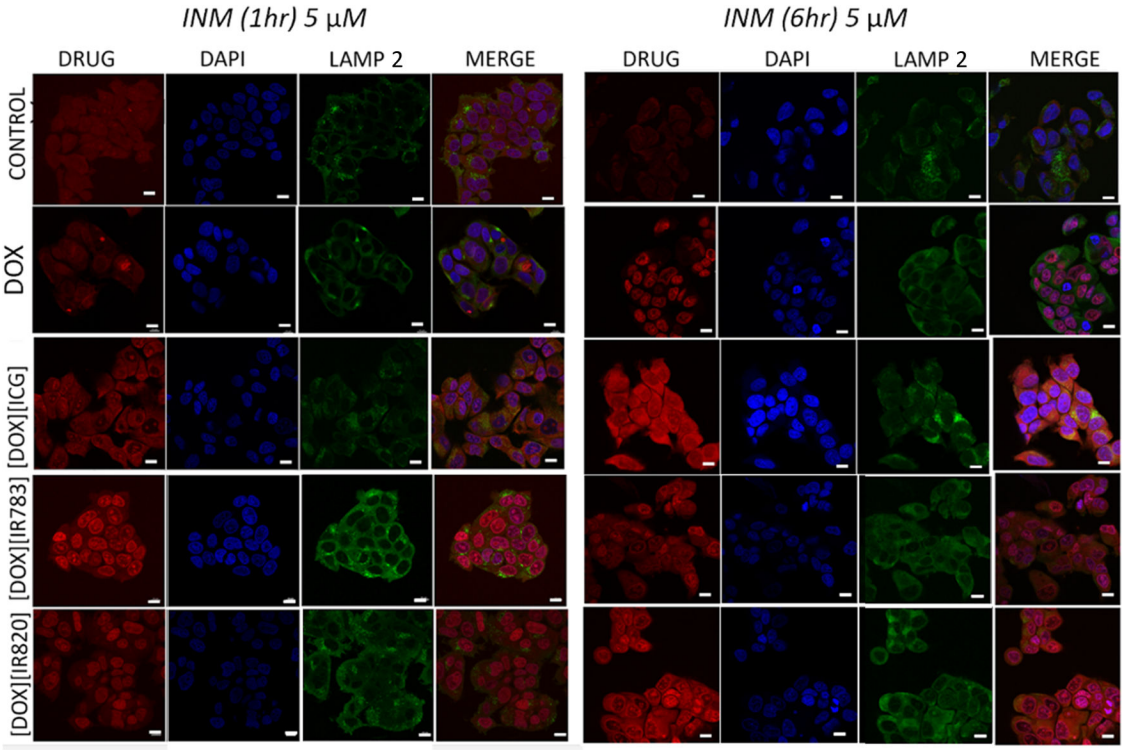

Figure 8.

Time-dependent subcellular localization (1 and 6 h) of MCF-7 cell lines treated with 5 μM DOX or chemo-PTT combination INMs, post-treated with DAPI and LAMP 2 antibodies. Scale bars represent 10 μm.

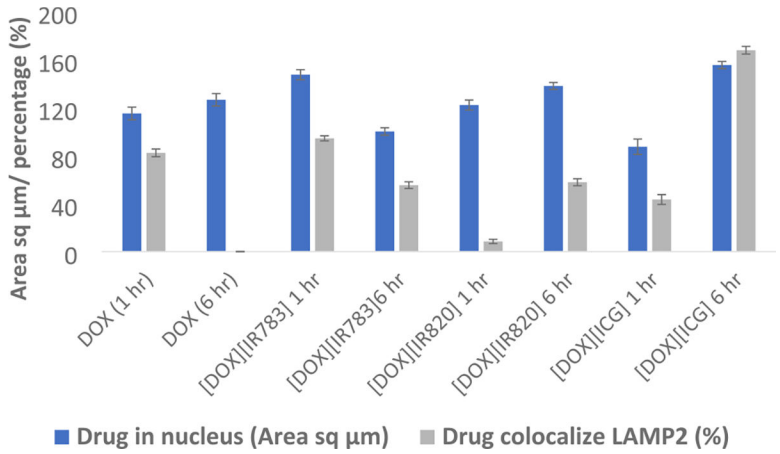

Figure 9.
Quantitative measurement of DOX and DOX-based INMs in the nucleus and LAMP 2.

Table 1.

Obstruction of Various Endocytosis Inhibitors and the Endocytosis Pathway

endocytosis inhibitor	pathway blocked	refs
chlorpromazine	CME, CVME	1,2,10,17
filipin III	CVME, CME	19,29,35
sucrose	macropinocytosis, CME	29
chloroquine	CME	29
imipramine	unclear mechanism, macropinocytosis	29
methyl-β cyclodextrin	CME, CVME	29
amiloride	CME, macropinocytosis	1,29